Macromolecules

Article

pubs.acs.org/Macromolecules

Probing Segmental Dynamics of Polymer Glasses during Tensile Deformation with Dielectric Spectroscopy

Jan Kalfus, Andrew Detwiler, and Alan J. Lesser*

Department of Polymer Science & Engineering, University of Massachusetts, Amherst, Massachusetts 01002, United States

ABSTRACT: An advanced broadband dielectric relaxation spectroscopy technique was developed to measure dipolar reorientation dynamics in an actively deforming amorphous polymer below the glass transition temperature. The application of a weak oscillating electric field during deformation allows for direct probing chain segment mobility. Results show that the application of a monotonically increasing strain on a glassy poly(vinyl chloride) induces a significant increase of the out-of-phase dielectric permittivity, thereby reflecting enhancement of the transition activity of chain segments. Moreover, the strain-dependent relaxation spectra suggest that the bifurcation of the relaxation processes decreases together with an overall increase in molecular mobility upon active deformation. The dielectric results also display a highly pronounced sensitivity to the apparent strain rate used for the mechanical excitation and isothermal aging prior to the deformation.

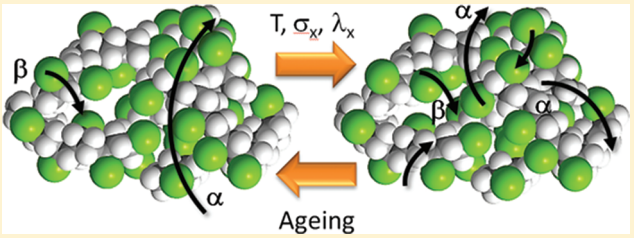

INTRODUCTION

A major factor inhibiting the development of reliable molecular models that accurately describe the deformation of polymer glasses is the lack of experimental data providing information about the molecular dynamics during the actual deformation. Currently, a number of researchers are developing models to predict the solid-state behavior of polymer glasses based on fundamental principles of polymer physics.[1−6] In contrast, there is very little experimental data available to evaluate these models. To date, the only available data that provide information with regard to molecular dynamics under an applied stress on glassy polymers include the work of Ediger and co-workers.[7,8]

In stark contrast, the rheology of polymer melts has evolved tremendously. This is due in large part to the development of innovative experimental techniques that provided information about molecular conformation and motions in the melt under a variety of systematic controlled flows as summarized in ref 9. One particularly relevant contribution to this paper is that of Wantanabe et al.,[10] who used the dielectric spectroscopy method to monitor the segmental mobility in the rheology of polymers above their T_g. These developments, in turn, led to significant advances in simulations and modeling of melts that inevitably enhanced understanding of the observed phenomena. Prior to these developments, the melt rheology dealt primarily with phenomenological models lending little ability to identify the underlying physics that relates molecular architecture of the melt to its associated properties.

In this contribution, we report on a new method to probe molecular mobility in glassy polymers during active deformation using dielectric spectroscopy. This paper illustrates the technique by deforming poly(vinyl chloride) (PVC) in uniaxial extension to relatively low strain levels (i.e., not far above the yield point of the glass). PVC was selected in this case because of the fact that the dipoles are rigidly attached to the backbone of the polymer. In this way, probing dipole dynamics are directly correlated to the polymer segmental dynamics. It should be emphasized that this approach employs a strong mechanical excitation exerted by the tensile test machine to produce mobility in the presence of a weak oscillatory electric field generated by the dielectric spectrometer to monitor changes in polymer chain segmental mobility arising from the application of a tensile stress (Figure 1). Using this approach,

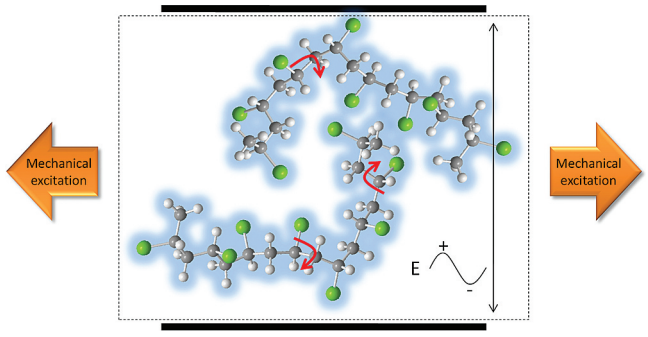

Figure 1. Scheme of uniaxially deformed polymer with dipoles rigidly attached to the chain backbone in an alternating electric field (E). An idealized rotational rearrangement of closely packed segments is sketched.

one can directly probe dynamics of dipolar rearrangement during the deformation. As will be presented below, the use of a broadband analyzer allows for measuring strain-dependent

Received: December 14, 2011
Revised: April 22, 2012
Published: May 23, 2012

dielectric tan δ documenting the effect of deformation on the polymer relaxation spectra. One of the key issues we address within this contribution is how the application of strain energy alters the segmental mobility of a glassy polymer as we approach yield and contrast that with how the mobility alters when we apply thermal energy and approach the glass transition temperature. We also probe how physical aging of the glass affects the segmental dynamics and investigate what effect the application of stress has on reversing this process.

EXPERIMENTAL SECTION

Materials, Processing, and Basic Characterization Methods. An extrusion grade of poly(vinyl chloride) (PVC, type I) containing no plasticizing additives was used. PVC was molded into 120 × 200 × 1 mm^3 sheets using a hot press at 190 °C and compressive force 20 kN. To minimize possible orientation of PVC chains during the molding process, a 5 min annealing period was applied after compressing. For cooling, a compressive force of 20 kN was applied with a separate water-cooled press. After the molding process, no segmental orientation was detected under crossed polars. Also, no coloration indicating presence of double bonds was noticed after the molding process. In addition, differential scanning calorimetry (DSC, Q200 TA Instruments) measurements of compression-molded PVC specimens were carried out in the temperature range from 0 to 190 °C, and no endotherm was found upon heating above the glass transition. Molecular characteristics of the compression-molded PVC material as obtained from the size exclusion chromatography measurements are shown in Figure 2 (Polymer Laboratories PL-GPC 50, THF solvent, column temperature 40 °C, 3 × PL Gel 5 μm mixed bead columns, refractive index detector).

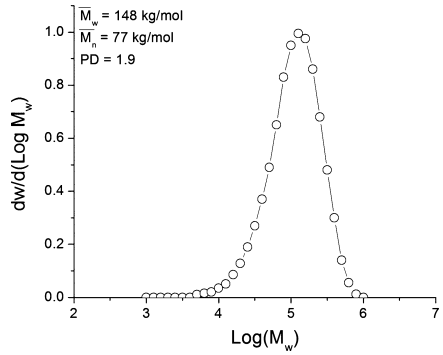

Figure 2. Distribution of molecular weights of PVC as obtained from the size-exclusion chromatography.

Prior to any mechanical and dielectric testing, the molded PVC material was conditioned in an air oven above T_g at 90 °C for 15 min, quenched to 20 °C, and then aged at the same temperature. Aging was done for the following periods of time: 0.25, 12, 24, and 720 h. Dynamic-mechanical properties were measured using a DMA Q800 (TA Instruments). Specimens 1 × 5 × 40 mm^3 used in the DMA experiments were punched out of compression-molded sheets.

Dielectric Spectroscopy. Dielectric spectroscopy represents a well-established relaxation technique operating either in the time domain or the oscillatory field regime. The Solartron SI 1260 analyzer used in this investigation was designed only for low-voltage oscillatory experiments operating in the frequency range 10^{-5}–10^{7} Hz. As mentioned above, high molecular weight PVC containing no plasticizing additives was used due to its suitable combination of dielectric and mechanical properties. In PVC, chlorine atoms, which are rigidly attached to the vinyl backbone, cause permanent distortion of electron density across the C−Cl bonds and create dipoles. These dipoles cannot travel freely across the sample between electrodes, and the dipolar diffusion represents a localized process which is strongly correlated to the dihedral mobility of the chain backbone. The dipolar reorientation occurring via the rotational isomerization is, therefore, the primary mechanism governing the dielectric relaxation response of PVC under conditions used in this study. The dielectric polarization of a material in a weak time-variable electric field can be generally expressed in a form, which is conceptually equivalent to Hooke's law used for describing mechanical perturbations:[11]

$$\varepsilon^*(\omega) \cong \frac{\mathbf{D}(\omega)}{\mathbf{E}(\omega)} \tag{1}$$

where $\varepsilon^*(\omega)$ is the dynamic dielectric permittivity, $\mathbf{D}(\omega)$ is the dielectric displacement, and $\mathbf{E}(\omega)$ is the electric field. The frequency-dependent permittivity can then be decomposed into the in-phase and the out-of-phase dielectric permittivity:

$$\varepsilon^*(\omega) = \varepsilon'(\omega) - i\varepsilon''(\omega) \tag{2}$$

The preceding relationship shows that the overall response to the oscillatory field (electric work done by the system) is composed of two distinct parts: stored in-phase and dissipated out-of-phase contribution. In other words, $\varepsilon'(\omega)$ represents that portion of the electric work which is absorbed and fully returned by the polymer during each cycle, while $\varepsilon''(\omega)$ pertains to the electric work returned in the form of heat. The dissipated part of the electric work is of particular interest due to its direct connection to the kinetics of the jump-overbarrier motions. Generally, the measure of the electric energy dissipation can be expressed as a ratio of the out-of-phase and the in-phase dielectric permittivity:

$$\tan\delta = \varepsilon''(\omega)/\varepsilon'(\omega) \tag{3}$$

Deformational Dielectric Spectroscopy. In the presented work, supercooled PVC is investigated with respect to the following three dynamically evolving situations: (i) a slow temperature ramp with constant heating rate, (ii) an isothermal aging at 20 °C, and (iii) a slow active deformation under isothermal conditions T = 20 °C. In all three cases, $\varepsilon'(\omega)$, $\varepsilon''(\omega)$, and tan δ were recorded to document the dynamics of segmental rearrangement.

The deformational dielectric experiments were carried out in a way that was in principle like any other dielectric measurements (circuit

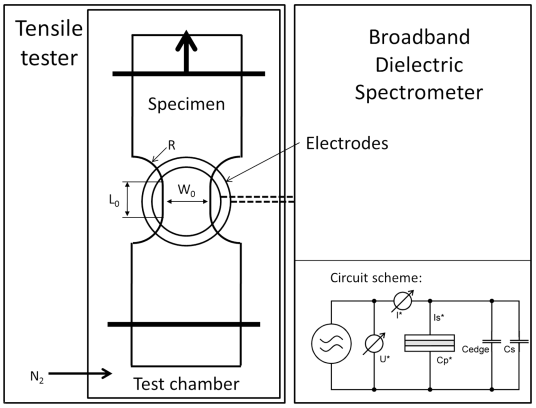

Figure 3. Scheme of the experimental setup.

scheme is included in Figure 3). A flat PVC specimen of a dog-bone shape was in contact with two parallel brass electrodes of circular shape. The specimen dimensions were modified in such a way that the gauge area was fully covered by the electrodes of the BDS: L_0 = 9.5 mm, W_0 = 11.5 mm, T_0 = 1 mm, R = 13 mm. As shown schematically in Figure 3, specimen ends were gripped in the strain-controlled universal tensile tester Instron 5800R, and an oscillatory electric field generated by the Solartron SI 1260 analyzer (part of the Novocontrol broadband dielectric spectrometer) caused displacement of dipoles. Consequently, the frequency-dependent dielectric permittivities were measured. In order to shield the electrodes and avoid air and moisture effects on the electric field between the two brass electrodes, ground

dx.doi.org/10.1021/ma202708j | Macromolecules 2012, 45, 4839–4847

custom-made aluminum chamber connected to a dry nitrogen purge with 100 mL/min was used. The test chamber contained ports for the upper and lower Instron clamps for gripping the sample. Mechanical excitation was carried out in uniaxial extension at various apparent strain rates defined as $d(L/L_0)/dt$: 5×10^{-4}, 5×10^{-5}, and 5×10^{-6} s^{-1}. One of the electrodes contained a built-in Pt100 thermocouple to measure possible temperature variations during the deformation, but no change of temperature was noticed under given conditions. A matrix of strain rates and preconditioning aging periods discussed in this contribution is shown in Table 1. Yield occurred at strains around $\lambda_x = 1.2$, where $\lambda_x = (L + L_0)/L$. In addition, a stress relaxation experiment was done at $\lambda_x = 1.2$ after each constant strain rate measurement. The dielectric response was measured simultaneously with the mechanical excitation using 1 V oscillatory electric field. Two brass electrodes were put in contact with specimen surface during the experiment using a steel frame with a screw for adjusting the position of the electrodes. The surfaces of the brass electrodes were polished by a sandpaper with grain size of 1 μm and wiped with clean paper tissue prior to each measurement. Note that the setup described in this paper can be used only below and at the material's yield point. Necking and strain localization cause significant material loss due to flow and electrode−specimen contact instability, leading to a pronounced decrease of tan δ.

Table 1. Matrix Scheme of Deformational BDS Tests[a]

	aging period (h)			
apparent strain rate (s^{-1})	0.25	12	24	720
5×10^{-4}	X	X		
5×10^{-5}	X	X		
5×10^{-6}		X	X	X

[a]PVC samples in different stage of aging done at 20 °C were uniaxially deformed with three different apparent strain rates.

RESULTS AND DISCUSSION

Relaxation Behavior of PVC. Amorphous PVC exhibits generally three main relaxation transitions: (i) a low-temperature secondary relaxation, (ii) a primary relaxation (glass transition), and (iii) a high-temperature terminal relaxation, which is related to the orientational homogenization (reptation motion) of entire chains. The nature of the primary and the secondary relaxation process in amorphous polymers has been studied by researchers for decades. In spite of the fact that many aspects of this phenomenon have been understood in an acceptable extent, some of them remain unanswered.[12,13] Generally, the transition of a polymer from a nonequilibrium to the equilibrium state exhibits a highly cooperative character. This cooperative transition is usually described as the primary or the α-relaxation process. At temperatures well below the primary relaxation process a less cooperative relaxation is usually detected, generally called the β-process. They both exhibit significant mechanistic connection between each other and will be expected to assist in the interpretation of the deformational BDS data.

A key factor that must be emphasized is the heterogeneous nature of segmental dynamics in a supercooled state. As the temperature decreases, the local packing effects start to dominate the segmental rearrangement, resulting in the correlated nearest neighbor and, particularly, the self-correlated "over-and-back" transitions as shown in atomistic computer simulations.[3,4,12] Active sites where these correlated events take place contain preferred configurational sequences which represent entities with high transition rates trapped among low mobility regions, hindering their diffusion along the chains. At sufficiently high temperatures, these highly mobile entities gradually cover longer parts of the chains and start to travel along them. Consequently, the size of the cooperatively rearranging region shrinks dramatically due to decreasing configurational restrictions.[14] Particularly, the interchain motional cooperativity is responsible for the fact that any change of segmental configuration is connected to the time scale that is dictated mainly by the activation entropy, which penalizes large segmental excursions. This can be generally expressed in terms of the Adam−Gibbs relation as follows:[14]

$$\ln \overline{\tau}_\alpha \propto \frac{\overline{\varepsilon}_\alpha}{k_B T} \frac{s^*_A}{S_C(T)} = \frac{\overline{\varepsilon}_\alpha}{k_B T} z^* \tag{4}$$

where $\overline{\varepsilon}_\alpha$ is the average activation energy reflecting the intramolecular energy landscape, s^*_A is the activation configurational entropy of a critical subsystem of size z^*, $k_B T$ corresponds to the kinetic energy of thermal motion, and $S_C(T)$ is the configurational entropy of the entire system. According to the Adam−Gibbs concept, the probability of an accidental accumulation of kinetic energy and consequent rearrangement somewhere in the system is governed by the critical size of the cooperatively rearranging region under given conditions of temperature, hydrostatic component of stress, thermal history, and other effects. The probability of a cooperative diffusion process is significantly lower than that belonging to a purely noncooperative transition state process. The configurational restrictions do not allow conformers to explore their reorientational space and the system becomes nonergodic under given conditions.

An example of the frequency−temperature dependence of the dielectric tan δ for rigid PVC specimen with no active deformation applied is presented in Figure 4a. It should be noted that both the α-relaxation process and the β-process are observed at the frequencies shown in Figure 4a. This will be contrasted later when strain energy is applied as opposed to thermal energy.

To document merging of both relaxation processes at elevated temperatures, a corresponding contour map diagram is shown in Figure 4b. In this plot, dark color corresponds to the low values of tan δ (valley) and bright color represents regions of high values of tan δ (peak). The two relaxation processes are significantly separated at low temperatures and begin to merge as the temperature increases. In addition, the absolute intensity of the β-process, as expected, increases and shifts to slightly higher frequencies with increasing temperature. The increase of the β-peak intensity is an indication that the concentration of localized high-mobility regions increases upon heating as well as the local constraint conditions change as temperature varies.

In Figure 5, a plot of the inverse temperature dependence of the frequency at tan δ peak maximum of the α-process and β-process, respectively, are presented. The mean potential energy hindering the dihedral motion calculated for the α-process is $\overline{\varepsilon}_\alpha$ = 14.5 ± 1 kJ/mol, which is slightly higher than the value corresponding to linear polyethylene[15] and the Vogel temperature, T_V, was 10 ± 2 °C.

$$\ln \overline{\tau}_\alpha = \ln \overline{\tau}^* + \frac{\overline{\varepsilon}_\alpha}{k_B T}\left(\frac{T}{T - T_V}\right) \tag{5}$$

The other limit is an extremely high temperature where the cooperativity of motional rearrangement disappears and the rate of rotational isomerization becomes equal to the mean

dx.doi.org/10.1021/ma202708j | Macromolecules 2012, 45, 4839−4847

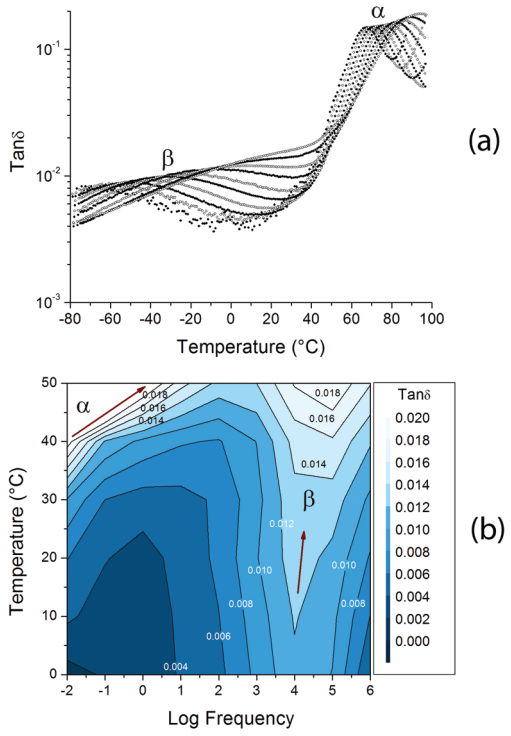

Figure 4. (a) Temperature-dependent dielectric tan δ measured at different frequencies. The glass transition temperature lies between 60 and 100 °C depending on the frequency of the oscillatory electric field. Low-temperature β-relaxation and high temperature α-relaxation process is indicated. (b) Corresponding contour map of the frequency−temperature-dependent dielectric tan δ is presented.

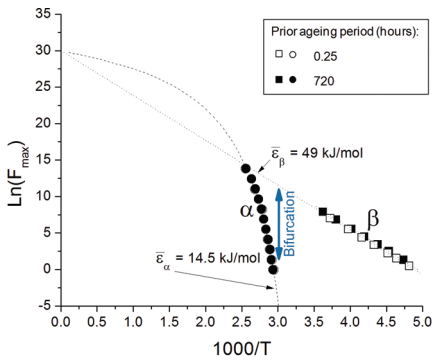

Figure 5. Relaxation map of PVC showing low-temperature bifurcation of the relaxation process.

frequency of vibrations, $1/\overline{\tau^*}$, being of the order of 10^{12} Hz.[16] It is also worth mentioning that any perturbation of the experimental time scale, due to a change of cooling rate or an isothermal aging step, can allow part of the spectrum of α-modes to be realized. This inevitably leads to a change of the T_V parameter used in eq 5. In Figure 5, no difference in the α-peak was observed for PVC regardless of its thermal history due to the slow heating rate used in the presented dielectric measurements −0.5 °C/min. A similar phenomenon is known in differential scanning calorimetry where the heat flow overshoot decreases with decreasing rate of heating and the inflection point shifts close to the response obtained for quenched polymer.[17]

The activation energy of the β-process was determined using the Arrhenius relation:

$$\ln \overline{\tau}_\beta = \ln \overline{\tau}^* + \frac{\overline{\varepsilon}_\beta}{k_B T} \quad (6)$$

The activation energy of the β-process $\overline{\varepsilon}_\beta$ = 49 ± 1 kJ/mol did not show any dependence on prior aging time at 20 °C. The aging caused only a minor shift of the β-peak toward lower temperatures.

The plot in Figure 5, however, does not represent true time−temperature superposition data. As seen from Figure 4, neither α- nor β-relaxation peak can be truly superposed due to the change of the peak intensity and, particularly in the case of the β-process, change of the peak width with increasing temperature. This phenomenon itself is not surprising and has been reported for other polymers.[9,18,19] The conformational dynamics are, as mentioned before, very sensitive to the temperature-dependent intermolecular correlations which become crucial at low temperatures.[12] From this point of view, the time−temperature superposition can be applied only when the distribution of relaxation times does not display a significant change upon heating or cooling. This is usually satisfied in a narrow temperature range at and above T_g.

Effect of Aging on Dielectric Spectra. Glassy polymers represent systems which are not in equilibrium and exhibit aging behavior. To illustrate this phenomenon, a mechanical aging trajectory of PVC obtained in dynamic-mechanical measurements under linear uniaxial strain oscillations is shown in Figure 6. Note that PVC rapidly stiffens at the beginning of the aging process—a linear change of E' requires logarithmic time scale.

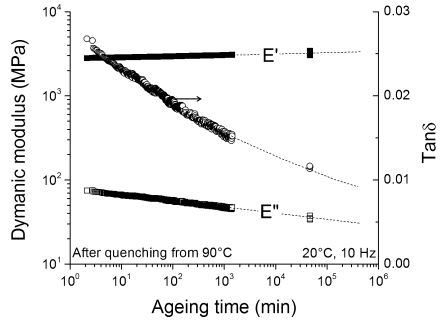

Figure 6. Mechanical aging trajectory of PVC at 20 °C after quenching from 90 °C.

Coarse dielectric relaxation spectra for PVC samples with different aging histories are presented in Figure 7. Two-dimensional and corresponding contour map plots are shown to better document bifurcation of the α- and β-relaxation process upon isothermal aging. Isothermal aging caused a very minor shift of the β-peak on the frequency scale, which is in agreement with results presented in Figure 5. On the other hand, the aging caused a noticeable decrease of the β-peak intensity and extended remarkably the gap between the α- and β-process. This bifurcation is in contrast to the results shown in Figure 5 due to the reasons already discussed above. The increase of the bifurcation and, particularly, decreasing β-peak upon isothermal aging clearly shows a non-Debye character of the supercooled PVC. As time proceeds during the isothermal aging, the α-mode motions occurring in the supercooled system eventually lead to the jamming of segments and tighter trapping of mobile regions. On the basis of the decrease of the β-peak intensity, one can speculate that the concentration of mobile

dx.doi.org/10.1021/ma202708j | Macromolecules 2012, 45, 4839−4847

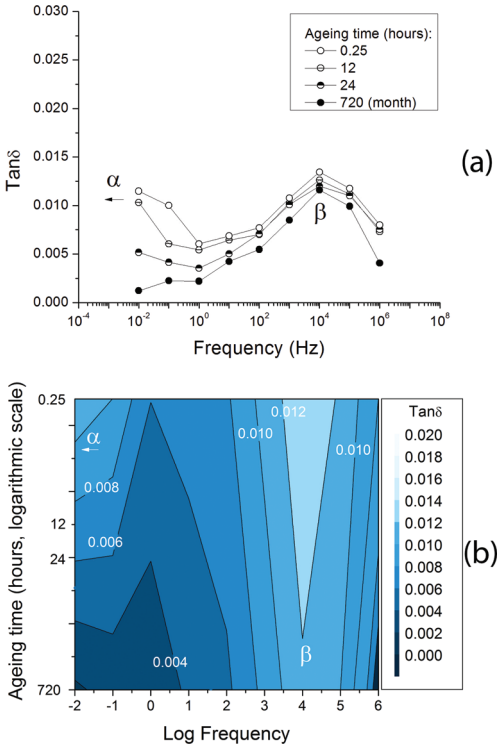

Figure 7. Frequency-dependent dielectric tan δ measured at 20 °C after quenching from 90 °C.

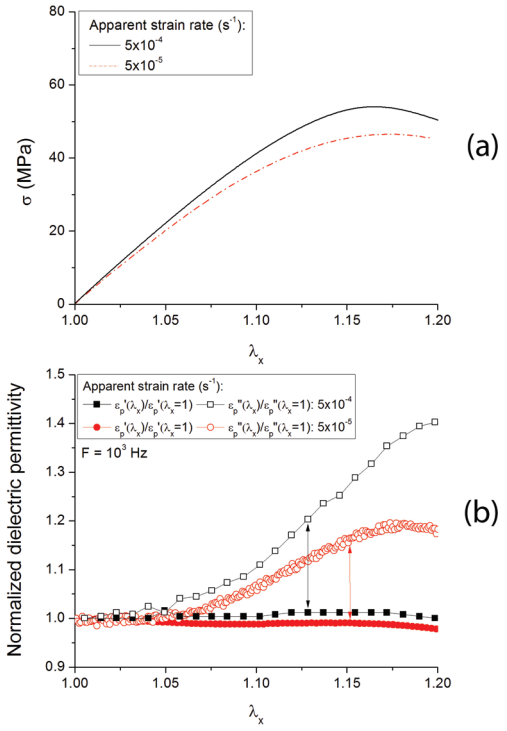

Figure 8. (a) Stress–strain curves obtained for PVC samples aged 12 h at 20 °C after quench from 90 °C. (b) Corresponding normalized dielectric permittivities measured at a frequency $F = 10^3$ Hz.

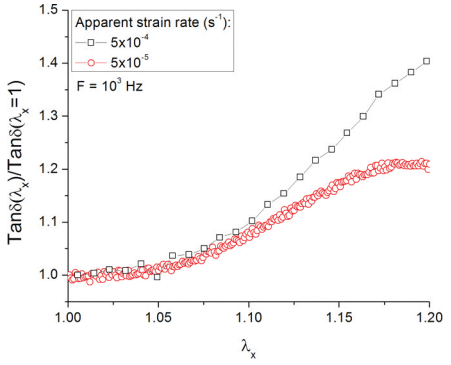

Figure 9. Normalized tan δ dependence on apparent strain measured at a frequency $F = 10^3$ Hz.

regions decreases upon isothermal aging as the overall segmental configuration becomes increasingly jammed. A qualitatively similar phenomenon has been shown in Figure 4b at low temperatures.

Effect of Deformation on Dielectric Response. From a macroscopic point of view, the response of an amorphous supercooled polymer to mechanical excitation exhibits a number of consecutive steps: (i) a linear regime, (ii) a nonlinear regime (inelastic deformation), (iii) instability (yield), (iv) inelastic flow followed by fracture. As seen in Figure 8a, the nonlinear regime is accompanied by a decrease of the stress–strain curve slope, which suggests that the material becomes less efficient at storing the elastic free energy. An increasing amount of the strain energy is dissipated due to the activated transition processes and the contribution of the elastic free energy component to the total free energy decreases during the deformation.

In Figure 8, mechanical stress–strain dependence and simultaneously measured dielectric permittivities are presented. As seen in Figure 8b, $\varepsilon''(\omega,\lambda_x)$ was noticeably more sensitive to the active deformation than $\varepsilon'(\omega,\lambda_x)$. In fact, more than 95% of the tan δ change upon active deformation was given by the change of the out-of-phase response, $\varepsilon''(\omega,\lambda_x)$. In Figure 9, the corresponding tan δ dependence upon increasing apparent strain is shown. A significant increase of the dielectric tan δ is observed at strains which correspond to the onset of the nonlinear stress–strain behavior, as shown Figure 8a. The strain-dependent dielectric permittivity exhibited also a highly pronounced sensitivity to the apparent strain rate.

Rutledge et al.[3,4] have simulated dynamics of rotational isomerization processes in an actively deforming supercooled system composed of united atom polyethylene chains under an N, P, T constraint. Long-range order was absent in the simulated system, and the chains displayed nonergodic behavior. Such a system was uniaxially compressed, and the rate of conformational transitions was calculated along with the mechanical stress. The simulated effect of active deformation on the bond transition activity is in agreement with the experimentally measured strain-dependent dielectric tan δ. The higher the strain rate the higher the transition rate and the dielectric tan δ. A closer analysis of the simulation data reveals that the percentage of trans conformations was only slightly increased in the range of strain $0.5-2 \times \lambda_x^{\text{yield}}$. This suggests that the deformation process below and around the yield point does not cause extreme deformation of the polymer coil domains. Moreover, in spite of the fact that the inelastic flow causes irreversible perturbation of segmental positions, the chain topology stays almost unaffected.[20] This is further supported by a simple experiment, where a supercooled glassy polymer deformed to or above the yield point is heated to a temperature close to its T_g for a short period of time and a 100% recovery is observed. This shows that the molecular

dx.doi.org/10.1021/ma202708j | Macromolecules 2012, 45, 4839–4847

interpenetration is generally not disturbed by the inelastic effects. Another result published by Rutledge et al.[3,4] showed that the nearest-neighbor correlation of conformational transitions significantly decreases upon deformation. This conclusion agrees well with the experimental results and analysis done by Ediger et al.[7] using a photobleaching relaxation technique. They analyzed rotational relaxation time distribution functions of bulky tracer molecules, whose dynamics are correlated to the surrounding polymer matrix. The distribution functions became narrower and shifted to shorter times during the inelastic flow process. This suggests that the time−strain or the time−stress superposition is not applicable as the material approaches the yield point and, more importantly, the reorientation dynamics become more homogeneous. The same conclusion has been made by Rottler et al.[6] based on coarse-grained computer simulations and Ediger et al.,[7] who measured reorientational dynamics of tracer molecules dissolved in glassy PMMA. It is worth noting that presented data have been obtained in measurements with controlled strain rate, while Ediger's approach is based on applying constant stress.

As seen in Figure 9, the portion of electric work dissipated due to the dipolar reorientation upon active deformation significantly increased with increasing apparent strain and strain rate. This measurement was done using oscillatory electric field with frequency $F = 10^3$ Hz. Such a frequency corresponded to the constrained dihedral jumps belonging to the slower side of the β-relaxation process. Figure 9 indicates that the transition rate is increased upon inelastic deformation, in agreement with data published by Rutledge et al.[3,4] It is important to note that the transition rate calculated by Rutledge et al.[3,4] displayed drop after stopping the deformation. In the deformational dielectric experiments, the strain-dependent tan δ exhibited a similar drop when the active deformation was stopped. This event was followed by a slow tan δ decay to the value, which was measured prior to the deformation. To document the decay of segmental mobility after stopping the deformation process, a simultaneously measured stress and tan δ relaxation data are shown in Figure 10. Drop of stress is followed by loss of dipolar mobility.

Aging Trajectory during Active Deformation. Figure 11a shows a nonlinear stress relaxation experiment done on a quenched PVC specimen. Two apparent strain rates were used for applying the uniaxial deformation prior to the relaxation experiment. The active deformation was stopped at uniaxial strain $\lambda_x = 1.20$, and the time-dependent stress was recorded. As

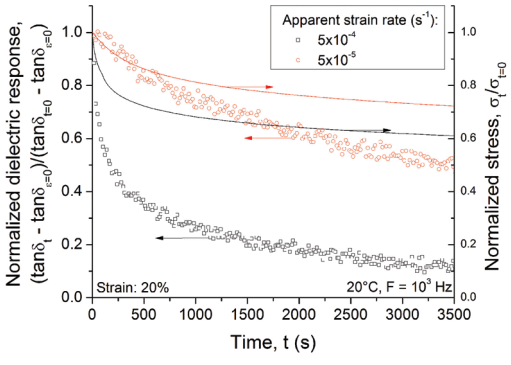

Figure 10. Normalized mechanical stress and normalized tan δ ($F = 10^3$ Hz) measured in dependence on time after reaching 20% of tensile strain.

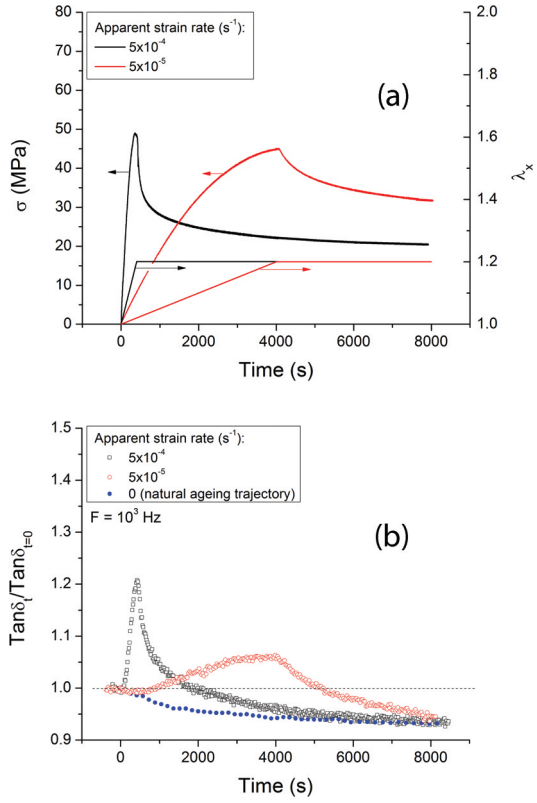

Figure 11. (a) Stress and apparent strain dependence on time measured for quenched PVC at 20 °C. The measurement is composed of two parts: (i) active deformation up to 20% strain and (ii) stress relaxation. (b) Corresponding tan δ dependences measured at $F = 10^3$ Hz. Aging trajectory of undeformed PVC sample was included for comparison.

seen in Figure 11b, significant aging process can be identified in the undeformed PVC specimen. Within the first hour of the isothermal aging a decrease by more than 5% of the original value of tan δ is observed. Therefore, deforming such a "fresh" PVC glass causes that the active deformation and the nonlinear stress relaxation take place simultaneously during the aging process.

In agreement with data presented above, the value of tan δ increases upon active deformation and its intensity is dictated by the apparent strain rate. As soon as the deformation is stopped, tan δ decays with an asymptotically decreasing rate documenting fading out of the segmental mobility in the PVC material as chain segments become jammed again. The most remarkable result is, however, that decreasing tan δ seems to asymptotically approach the natural aging trajectory measured for the undeformed PVC specimen. The mechanical perturbation can cause a perturbation of previous thermal history of a supercooled polymer, but this effect seems to be only a temporary one and the glassy polymer asymptotically approaches the state of low segmental mobility immediately after the active deformation was stopped. This is in agreement with photorelaxation results published by Ediger et al.[7] Supposing that the chain topology was not perturbed upon deformation, the subsequent aging process should proceed to a reference state which is close to that of the undeformed polymer.

Deformation of Aged PVC. To obtain a deeper insight into the effect of mechanical perturbation on the motional

dx.doi.org/10.1021/ma202708j | Macromolecules 2012, 45, 4839−4847

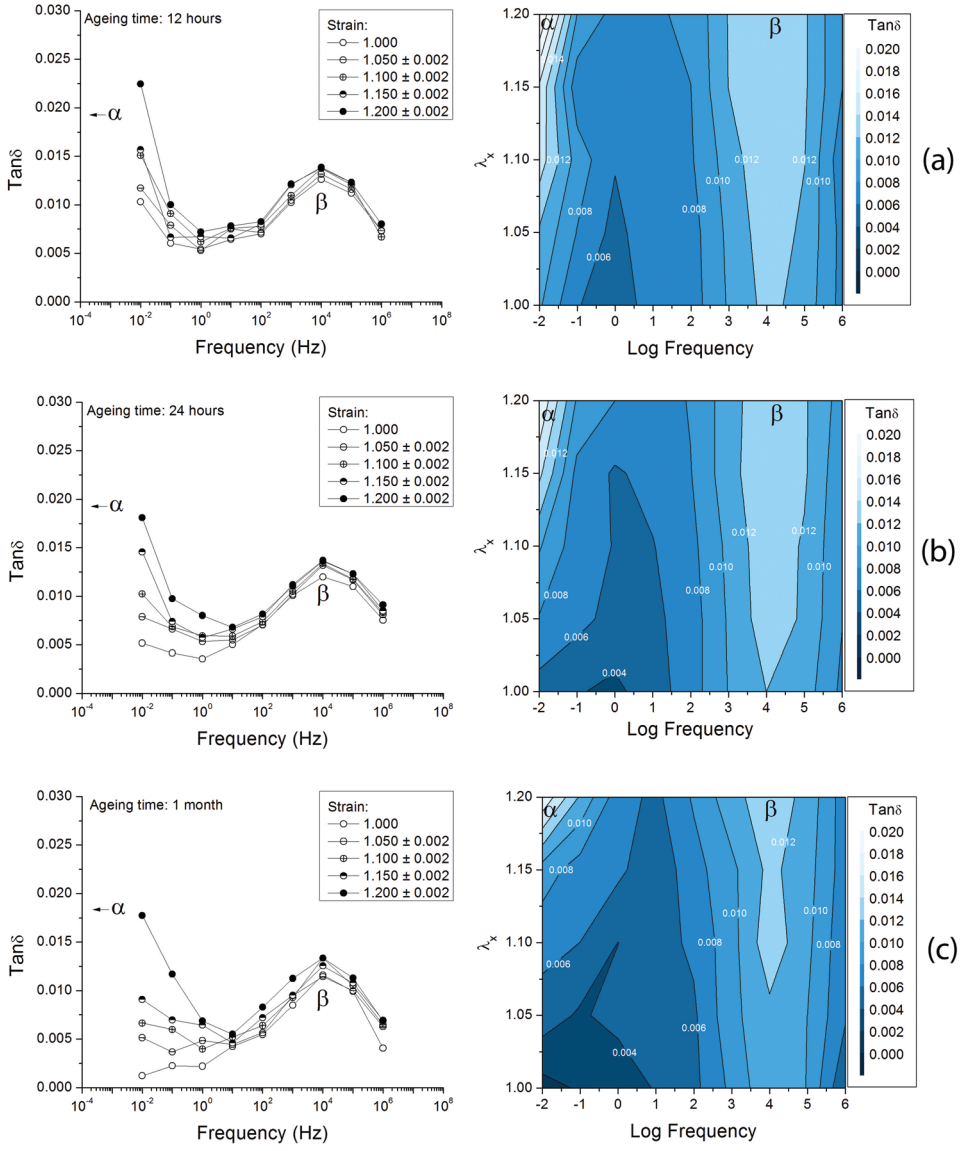

Figure 12. Frequency-dependent dielectric tan δ measured at 20 °C during active deformation at apparent cross-head speed 5×10^{-5} s^{-1}. Graphs represent data obtained after three different aging periods prior to measurement: (a) 12, (b) 24, and (c) 720 h. Classical two-dimensional plots are on the left, and the corresponding contour maps are on the right.

cooperativity of chain segments, a series of plots of strain and frequency dependent tan δ are shown in Figure 12. Plots a–c differ only in the amount of time of isothermal aging of PVC specimens prior to the deformation. To allow at least partial capturing of the α-relaxation process, which started to occur at frequencies much lower than 1 Hz, a very low apparent strain rate (5×10^{-6} s^{-1}) was used for the uniaxial deformation to allow for applying a broader frequency range, 10^{-2}–10^{6} Hz. The duration of one frequency sweep corresponded to a change of strain $\Delta\lambda_x$ slightly less than 0.002. As seen in Figure 12, the α–β bifurcation at $\lambda_x = 1$ increases, from (a) to (c), which corresponds to increasing periods of isothermal aging prior the experiment. On the other hand, the frequency gap between the α- and β-relaxation shows a tendency to decrease upon active deformation. In Figure 13, a comparison of the frequency-dependent tan δ measured at $\lambda_x = 1.2$ demonstrates that the frequency–tan δ dependences for PVC samples with different aging times merged under given conditions of active deformation.

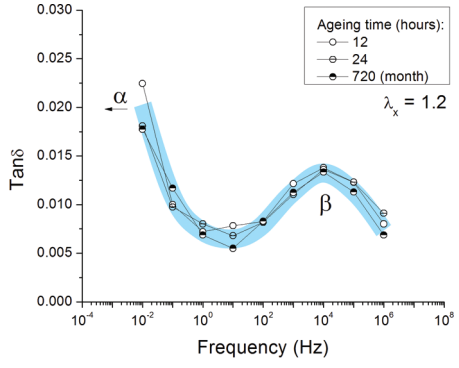

Figure 13. Frequency-dependent dielectric tan δ measured at 20 °C during active deformation at 20% of strain achieved at apparent strain rate of 5×10^{-5} s^{-1}.

A number of very interesting phenomena appear in the results presented in Figures 12 and 13. First of all, the α–β bifurcation noticeably decreases due to the apparent shift of the

dx.doi.org/10.1021/ma202708j | Macromolecules 2012, 45, 4839–4847

α-relaxation to higher frequencies upon active deformation as shown schematically in Figure 14. These data suggest that the

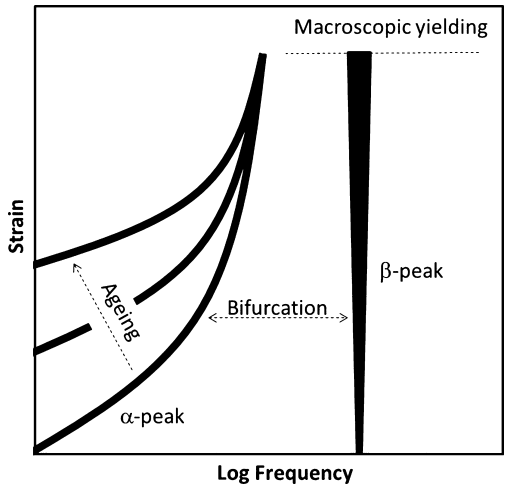

Figure 14. Sketch of the effect of strain on the α- and β-process.

cooperativity mechanism of the α-modes is appreciably altered at high stresses/strains. Not only the energy barriers are effectively decreased due to the mechanical excitation, but also a breakup of cooperatively rearranging domains takes place under high stresses/strains.[16] Another important aspect of the observed phenomenon is that the β-peak intensity increases upon deformation. This implies that the trapping of localized regions of higher segmental mobility decreases, leading effectively to the increase of population of actively rotating backbone bonds. In general terms, the deformation process exhibits some attributes of a reverse aging process or thermally induced devitrification. Using the term "mechanical rejuvenation" is also appropriate, but one has to bear in mind that this process is exclusively coupled to the high levels of mechanical excitation under given conditions of temperature, hydrostatic component of stress, etc. The postdeformation state is characteristic of mobility decay toward the natural aging trajectory, as shown before.

The above results inevitably raise a question regarding applicability of the Eyring concept[21] for describing inelastic flow in supercooled polymers. This classic concept of reaction rates has been used in many modifications to describe the inelastic flow in glassy polymers. The original model, as published in 1936, was established for simple atomic or molecular liquids under appropriate limiting conditions. This classic concept models the impact of mechanical stress on the relaxation time and viscosity of a material in such a way that the stress decreases effectively the free energy barriers associated with the diffusive motion of molecules. This concept has then been used by Tobolsky et al.,[22] where the effect of mechanical excitation on the free energy landscape has been established in the approximate one-dimensional form:[21]

$$\frac{\Delta G^*}{2}\left(1 - \cos\frac{2\pi\xi}{\delta}\right) - \xi\phi \tag{7}$$

where ΔG^* is the activation free energy, ξ is the motional coordinate, and δ is the distance between successive equilibrium positions. The mechanical perturbation is included in the linear term $-\phi\xi$, where ϕ is the force applied to a molecular unit. The Eyring–Tobolsky model has been established for situations where the condition of low mechanical perturbation, $\phi\xi \ll \Delta G^*$, is fulfilled.[21] With respect to the relaxation data presented in this contribution, it is important to emphasize that the above model does not treat explicitly the activation entropy needed for the cooperative rearrangement of chain segments and its strain/stress dependency. The entropy is generally a part of the free energy potential, but the effect of the external mechanical perturbation on the entropy term has not been established yet. The configurational restrictions affect not only the height of the free energy barriers, but it is reasonable to assume that they have profound effect on the shapes of the free energy barriers. More explicitly, a chain segment displacement need a cooperative action of the neighboring segments which itself requires a significantly longer reaction coordinate. Apparently, the parameter z^* used in eq 4 must then be a function of the mechanical excitation. In terms of the Adam–Gibbs concept,[12] the effect of mechanical excitation on the free energy barrier can schematically be expressed as[16]

$$\frac{\overline{\varepsilon}_\alpha}{k_B T}\left[\left(\frac{s^*_A}{S_C}\right)_{\phi\xi} - \left(\frac{s^*_A}{S_C}\right)_{\phi\xi=0}\right] \tag{8}$$

On one hand, the above term provides a reasonable conceptual framework showing that the mechanical excitation causes breakdown of cooperative domains (shift of the α-relaxation to higher frequencies). On the other hand, it is not directly applicable for the Eyring–Tobolsky model.[22] Data presented in Figure 12 show that there is a spectrum of cooperatively rearranging regions in the supercooled PVC with different mobilities. It is reasonable to assume that each of these regions responds to the applied excitation in a different manner. The issue of local response has been addressed and analyzed by Ediger et al.[7] They clearly showed that the mechanical perturbation narrows the distribution of relaxation times measured for tracer molecules dispersed in a supercooled matrix. The relaxation time spectra became narrower upon the mechanical perturbation and displayed shift to shorter times, which is in agreement with data shown in Figure 12. Thus, the jammed low mobility regions possess different sensitivity to the external mechanical perturbation compared to the domains of higher mobility. Ediger et al.[3,4] have also compared the effects of temperature and stress on the distribution of relaxation times and showed that the mechanical and thermal rejuvenation are not truly equivalent. These circumstances are not explicitly included in the Eyring–Tobolsky model.[22]

The Eyring–Tobolsky model captures the basic molecular mechanism of inelasticity in supercooled polymers correctly. As schematically summarized in Figure 14, mechanical excitation causes shift of the α-modes toward higher frequencies and increases intensity of the β-modes, which reflects increase of segmental mobility. What is not captured by the Eyring–Tobolsky model[22] is homogenization of the segmental dynamics. Thus, it can be concluded that the Eyring–Tobolsky model[22] provides only a framework approach, where the problematic circumstances, such as the polymer relaxation spectrum and complexity of atomic trajectories, are neglected. To extend the Eyring–Tobolsky model,[22] one would have to include both distribution of local mechanically induced relaxatory motions and precise knowledge of the mechanism, which transforms the macroscopic mechanical perturbation into the local displacements of discrete atoms. These are, however,

dictated by the local constraint conditions. Currently, these circumstances seem to be too severe to allow for developing analytical model able to fully capture the complexity of the inelastic flow in supercooled polymers.

SUMMARY

The primary goal of this work was to develop an advanced broadband dielectric spectroscopy method which would be capable of revealing fundamental aspects of inelastic deformation in supercooled PVC. In uniaxially stretched PVC, more than 95% of the strain-dependent dielectric tan δ was caused by the change of the out-of-phase dielectric permittivity. Such tan δ increase was not permanent and exhibited relaxation toward the unstrained value during the stress relaxation experiment. The strain-induced tan δ increase corresponded to the enhanced rate of dipolar reorientation realized via the activated transition state processes occurring in the PVC chain backbone. The strain-dependent tan δ was sensitive to the strain rate and has been shown to be asymptotically decaying toward the value measured for the unstrained PVC material.

The second important goal of this paper was to find a correlation between thermal rejuvenation, mechanical rejuvenation, and isothermal aging. Supercooled PVC exhibited heterogeneous segmental dynamics at temperatures below 110 °C where bifurcation between the α- and β-relaxation processes was observed. Such a bifurcation was found to be increasing upon isothermal aging, thereby showing that the aging process enhances heterogeneity of the segmental dynamics. The active deformation caused noticeable decrease of the $\alpha-\beta$ bifurcation. This effect was particularly strong close to the yield point. This result is in agreement with the works published by Ediger et al.[7] and Rutledge et al.[3,4] The active deformation caused segmental dynamics to become more homogeneous compared to the unstrained PVC. In this respect, the deformation process exhibits some aspects of a thermally induced devitrification process or an isothermal aging process running with a reverse arrow of time.

AUTHOR INFORMATION

Notes

The authors declare no competing financial interest.

ACKNOWLEDGMENTS

The authors are very grateful to Professor W. J. MacKnight (UMass) for motivating discussions at the beginning of the project and providing the Novocontrol broadband dielectric spectrometer. The authors highly appreciate friendly discussions with Professor S. S. Sternstein (RPI), Professor K. Nelson (RPI), and Professor R. Stein (UMass). Help provided by Ph.D. students Naveen Singh and Angela Cugini is acknowledged.

REFERENCES

(1) Chen, K.; Saltzman, E. J.; Schweizer, K. S. *Annu. Condens. Matter Phys.* **2010**, *1*, 277.
(2) Riggleman, R. A.; Lee, H.-N.; Ediger, M. D.; de Pablo, J. J. *Soft Matter* **2010**, *6*, 287.
(3) Capaldi, F. M.; Boyce, M. C.; Rutledge, G. C. *Polymer* **2004**, *45*, 1391.
(4) Capaldi, F. M.; Boyce, M. C.; Rutledge, G. C. *Phys. Rev. Lett.* **2002**, *89*, 175505.
(5) Adolf, D. B.; Chambers, J. M.; Caruthers, J. M. *Polymer* **2004**, *45*, 4599.
(6) Warren, M.; Rottler, J. *J. Chem. Phys.* **2010**, *133*, 164513.
(7) Lee, H.-N.; Ediger, M. D. *Macromolecules* **2010**, *43*, 5863.
(8) Lee, H.-N.; Paeng, K.; Swallen, S. F.; Ediger, M. D.; Stamm, R. A.; Medvedev, G. A.; Caruthers, J. M. *J. Polym. Sci., Part B: Polym. Phys.* **2009**, *47*, 1713.
(9) Strobl, G. *The Physics of Polymers: Concepts for Understanding Their Structure and Behavior*; Springer: Berlin, Germany, 2007.
(10) Matsumiya, Y.; Watanabe, H.; Inoue, T.; Osaki, K. *Macromolecules* **1998**, *31*, 7975.
(11) Bartenev, G. M. *Relaxation Phenomena in Polymers*; Wiley: London, UK, 1974.
(12) Smith, G. D.; Bedrov, D. *J. Polym. Sci., Part B: Polym. Phys.* **2007**, *45*, 627.
(13) Donth, E. *The Glass Transition: Relaxation Dynamics in Liquids and Disordered Materials*; Springer: Berlin, Germany, 2001.
(14) Adam, G.; Gibbs, J. H. *J. Chem. Phys.* **1965**, *43*, 139.
(15) Miller, A. A. *Macromolecules* **1978**, *11*, 859.
(16) Matsuoka, S. *Relaxation Phenomena in Polymers*; Hanser: Munich, Germany, 1992.
(17) Hodge, I. M. *Macromolecules* **1983**, *16*, 898.
(18) Runt, P. J.; Fitzgerald, J. J. *Dielectric Spectroscopy of Polymeric Materials: Fundamentals and Applications*; American Chemical Society: Washington, DC, 1997.
(19) McCrum, N. G.; Read, B. E.; Williams, G. *Anelastic and Dielectric Effects in Polymeric Solids*; Wiley: London, UK, 1967.
(20) Brown, D.; Clarke, J. H. R. *Macromolecules* **1991**, *24*, 2075.
(21) Eyring, H. *J. Chem. Phys.* **1936**, *4*, 283.
(22) Tobolsky, A. V.; Andrews, R. D. *J. Chem. Phys.* **1945**, *13*, 3.